

Strain effects in spinel ferrite thin films from first principles calculations

Daniel Fritsch and Claude Ederer

School of Physics, Trinity College Dublin, Dublin 2, Ireland

E-mail: fritschd@tcd.ie

Abstract. The *inverse* spinel ferrimagnets CoFe_2O_4 (CFO) and NiFe_2O_4 (NFO) are of interest for applications in spin-filter devices or as building blocks of artificial multiferroic heterostructures. Here we present density functional theory calculations of the structural and magnetic properties of CFO and NFO, with special emphasis on strain-induced changes in the magneto-crystalline anisotropy energy. We find that tensile (compressive) strain favours perpendicular (in-plane) anisotropy, in agreement with experimental observations. Our calculated magnetostriction constants λ_{100} agree well with available experimental data. Furthermore, the influence of different cation arrangements used to represent the *inverse* spinel structure and the effect of different exchange-correlation functionals are analysed and discussed.

1. Introduction

CoFe_2O_4 (CFO) and NiFe_2O_4 (NFO) are room-temperature insulating ferrimagnets with high Curie temperature and large saturation magnetisation which makes them promising candidates for applications in spin-filter devices or as building blocks of artificial multiferroic heterostructures [1, 2].

For all these possible applications the spinel ferrites have to be grown on suitable substrates, which usually incorporate strain into the thin film material. This strain can have a strong influence on the structural and magnetic properties of the grown structures. It has been shown experimentally for CFO that, depending on growth conditions and substrate treatment, a reorientation of the magnetic easy-axis can be observed [3, 4]. Furthermore, a strong enhancement of magnetisation and conductivity has been reported in NFO [2]. From the experimental point of view it is not clear whether the observed deviations from bulk behaviour are determined solely by the strain incorporated in the thin films or whether there are growth-related influences such as defects, off-stoichiometry, or interface effects responsible for these deviations. Density functional theory (DFT) calculations are able to address these effects separately, and therefore provide valuable insights in these materials. Here we present results of DFT calculations for the structural and magnetic properties of epitaxially strained CFO and NFO, with special focus on strain-induced changes in the magneto-crystalline anisotropy energy (MAE). Our results, which are representative for (001)-oriented thin films of CFO and NFO grown on different lattice-mismatched substrates, are important for further interpretation of experimental observations in thin films and heterostructures containing spinel ferrites.

2. Computational details

The *inverse* spinel structure (space group $Fd\bar{3}m$, general formula AB_2O_4) contains two inequivalent cation sites, the tetrahedrally-coordinated A -site (T_d), occupied in the present case by Fe^{3+} cations, and the octahedrally-coordinated B -sites (O_h), occupied by randomly distributed Fe^{3+} and Co^{2+} (or Ni^{2+}) cations. Experimental observations show that both Fe^{3+} and Co^{2+} are in their high-spin states, and that the magnetic moments of the A -site cations are oriented antiparallel to the magnetic moments of the B -site cations (so-called Néel-type ferrimagnetic arrangement) [5]. Thus, the magnetic moments of the trivalent Fe^{3+} cations on the A - and B -sites cancel each other out and the net magnetisation is determined by the divalent cation (Co^{2+} or Ni^{2+}), resulting in magnetisations close to the formal values of $3 \mu_B/f.u.$ and $2 \mu_B/f.u.$ for CFO and NFO, respectively. In an early work, Penicaud *et al.* [6] performed DFT calculations within the local-spin density approximation (LSDA) for magnetite Fe_3O_4 as well as for Co-, Ni-, Mn-, and Zn-substituted ferrites. These calculations yielded a half-metallic ground-state (except for NFO), in contrast to the experimentally observed insulating ground-state. It was later shown that applying the LSDA+ U approach to Co-, Ni-, and Mn-substituted Fe_3O_4 yields an insulating solution [7].

Here we present and compare results obtained within the LSDA, the generalised gradient approximation (GGA), the LSDA+ U , and the GGA+ U approach. All calculations have been performed using the “Vienna Ab-Initio Simulation Package” (VASP) [8, 9], and standard PAW potentials supplied with VASP. A plane wave energy cutoff of 500 eV and a Γ -centred $5 \times 5 \times 5$ k -point grid ensured converged results for the structural relaxations. The Hubbard U correction has been applied using the simplified, rotationally invariant version according to Dudarev *et al.* [10], and an effective $U_{\text{eff}} = U - J = 3$ eV has been used for all transition metal cations.

As discussed above, the divalent and trivalent cations are randomly distributed across the octahedrally-coordinated B -sites of the *inverse* spinel structure in both CFO and NFO. For our calculations, which are performed within periodic boundary conditions, we have to choose a specific cation arrangement. Here we use the smallest possible unit cell containing four B -sites, which leads to an artificial symmetry lowering from space group $Fd\bar{3}m$ to $Imma$. The resulting geometry consists of alternating planes of either Fe^{3+} or Co^{2+} (Ni^{2+}). Depending on the specific choice made, these planes can be oriented perpendicular to the x , y , or z direction, leading to three “settings”, which are completely symmetry-equivalent in the unstrained case. If the unit cell is strained, the settings become inequivalent, depending on whether the cation planes are parallel or perpendicular to the “substrate” plane. Comparing results obtained for different settings allows us to estimate the effect of different cation arrangements on the strain-dependent properties.

To minimise the influence of the artificial symmetry lowering on the results, we have applied the following constraints during the structural relaxations. For the unstrained bulk-like structures the lattice constants are constrained to be equal in all three directions, i.e. $a = b = c$, and the A -site cations are fixed to their ideal cubic positions. All other coordinates are relaxed at different volumes, and then the volume that minimises the total energy is identified. For the strained structures, the two in-plane lattice constants are constrained to be equal (epitaxial strain) and the out-of-plane lattice constant and all internal parameters are relaxed.

Once the structural properties of the strained structures have been determined by scalar-relativistic calculations, spin-orbit coupling is switched on and the total energies for different orientations of the magnetisation are calculated. We define the MAE as energy difference for orientation of the magnetisation along $[hkl]$, relative to the orientation parallel to the $[001]$ direction, i.e. $E_{\text{MAE}}(hkl) = E_{001} - E_{hkl}$.

Table 1. Optimised bulk lattice constants a_0 , bulk moduli B , 2-dimensional Poisson ratio ν_{2D} , and elastic constants C_{11} and C_{12} for CoFe_2O_4 and NiFe_2O_4 , calculated using the LSDA, LSDA+ U , GGA, and GGA+ U exchange-correlation functionals in comparison with experimental data.

	CoFe_2O_4					NiFe_2O_4				
	a_0 [Å]	B [GPa]	ν_{2D}	C_{11} [GPa]	C_{12} [GPa]	a_0 [Å]	B [GPa]	ν_{2D}	C_{11} [GPa]	C_{12} [GPa]
LSDA	7.951	475	—	—	—	7.949	847	—	—	—
LSDA+ U	8.231	206	1.19	282	168	8.196	213	1.17	295	172
GGA	8.366	211	—	—	—	8.346	166	—	—	—
GGA+ U	8.463	172	1.14	241	138	8.426	177	1.11	252	140
Exp. (Ref. [13])	8.392	186	1.17	257	150	8.339	198	1.18	273	161

3. Results and discussion

3.1. Structural properties

The lattice constants and bulk moduli of CFO and NFO calculated using different exchange-correlation functionals are listed in table 1. It can be seen that LSDA leads to a very large underestimation of the lattice constant of $\sim 5\%$, and an extremely large overestimation of the bulk modulus. All other functionals lead to a much better agreement with the experimental values for both lattice constants and bulk moduli. We note that even though GGA leads to excellent agreement with the experimental lattice constants, the bulk moduli obtained by both LSDA+ U and GGA+ U are closer to the experimental values than the pure GGA result. Overall, the deviations from the experimental values obtained within GGA, LSDA+ U , and GGA+ U are within the typical errors of these functionals for transition metal oxides [11, 12].

The densities of states (DOS), calculated using different exchange-correlation functionals for CFO and NFO are shown in figure 1. It can be seen that within LSDA both the majority- and minority-spin t_{2g} -states of the Co^{2+} cations are completely filled, whereas the corresponding majority spin e_g -states are only partially filled. This indicates a low-spin configuration of Co^{2+} , in contrast to the experimentally observed high-spin state. Similarly, LSDA also leads to a low-spin configuration of the B -site Fe^{3+} cations (not shown). Due to the much smaller ionic radius of the low-spin cations compared to the corresponding high-spin cations, the lattice constants for both CFO and NFO are severely underestimated within LSDA. This failure of LSDA has already been reported previously for NFO [14].

Pure GGA leads to the correct high-spin state of Co^{2+} (and Fe^{3+}), but still yields a half-metallic solution for CFO, with the Fermi energy cutting through the minority spin Co t_{2g} -states, and only a very small energy gap for NFO. Applying the Hubbard U correction splits the occupied and unoccupied transition metal d -states and shifts them well below and above the Fermi energy (LSDA+ U and GGA+ U panels), yielding the correct insulating ground-state for both spinel ferrites. It appears that both LSDA+ U and GGA+ U are equally well suited for a reliable description of structural and magnetic properties of spinel ferrites, and in the following we usually report and compare the results obtained by both methods.

The 2-dimensional Poisson ratio ν_{2D} (which relates in-plane and out-of-plane strain via $\varepsilon_{zz} = -\nu_{2D}\varepsilon_{xx}$), and the cubic elastic constants C_{11} and C_{12} [15], obtained from the strain-dependent relaxations described in the previous section, are listed in table 1 for both LSDA+ U and GGA+ U . The corresponding values are in good agreement with available experimental data (within the typical accuracy).

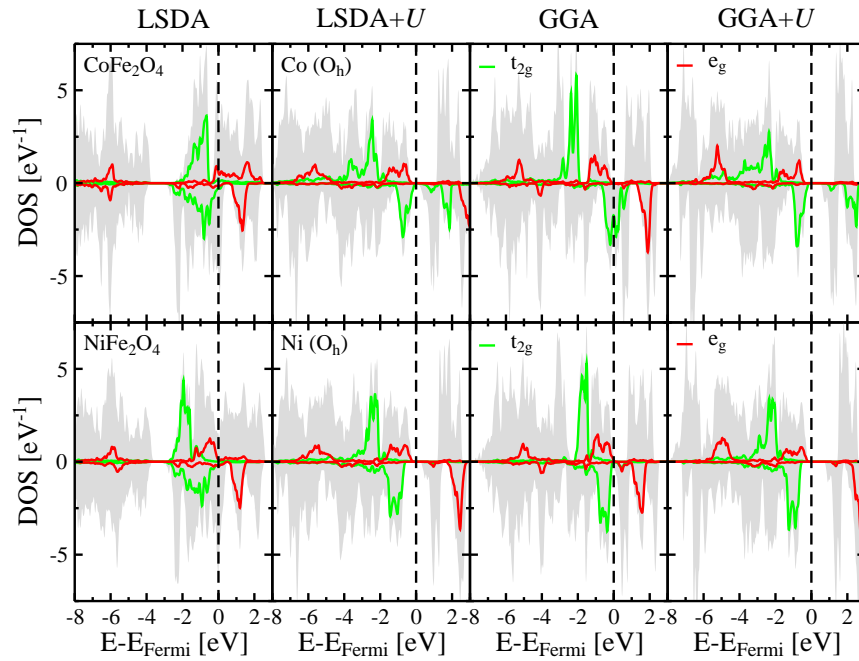


Figure 1. Total and projected DOS per formula unit for CoFe_2O_4 (upper panels) and NiFe_2O_4 (lower panels). The d states of Co and Ni (O_h) are separated into t_{2g} (green) and e_g (red) contributions. From left to right the influence of different exchange-correlation functionals (LSDA, LSDA+ U , GGA, GGA+ U) is shown. The total DOS is shown as shaded grey area in all panels. Majority (minority) spin projections correspond to positive (negative) values.

3.2. Magnetoelastic properties

Figure 2 shows the effect of strain on the MAE calculated for CFO (GGA+ U (a)) and NFO (LSDA+ U (b) and GGA+ U (c)), respectively. It can be seen that tensile (compressive) strain generally favours perpendicular (in-plane) orientation of the magnetisation, in agreement with experimental observations [3, 4]. From the slope of the data shown in figure 2 we can determine the magnetoelastic coupling constant B_1 [15]. Together with the elastic constants (table 1)

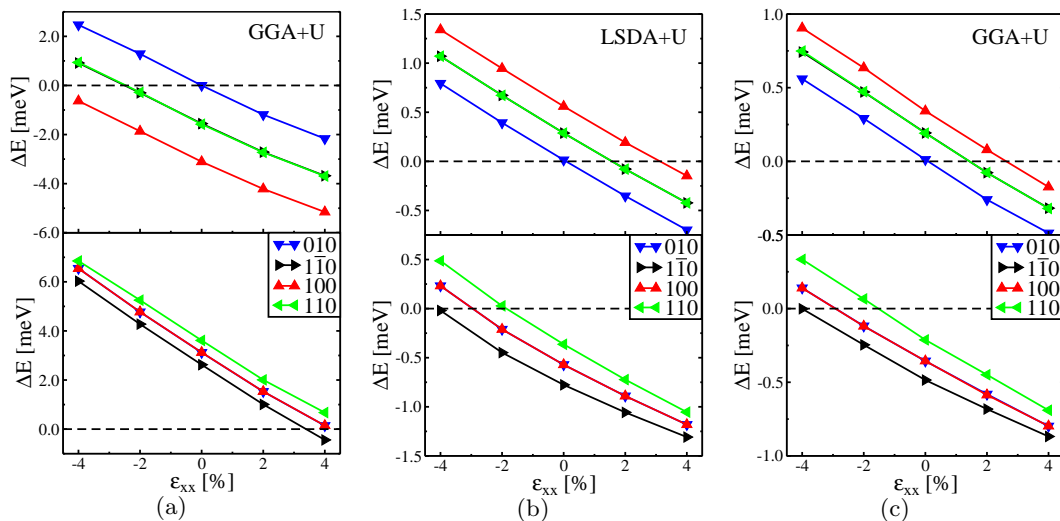


Figure 2. Total energy differences for different orientations of the magnetisation with respect to the [001] direction for CFO (GGA+ U (a)) and NFO (LSDA+ U (b) and GGA+ U (c)). Upper (lower) panels show results for perpendicular (in-plane) orientation of the Fe^{3+} and Co^{2+} (Ni^{2+}) planes with respect to strain plane.

this gives access to the magnetostriction constant $\lambda_{100} = -2B_1/[3(C_{11} - C_{12})]$, which is readily accessible from experiments (see Refs. [15] and [16] for more details).

The LSDA+ U calculations for NFO yield values for λ_{100} of -55 ppm and -52 ppm for “settings” 1 and 3, respectively, whereas GGA+ U yields slightly lower values of -40 ppm and -36 ppm. Thus, the influence of the specific cation arrangement is smaller than the uncertainty due to the different exchange-correlation functions. All values are in good agreement with available experimental data, which ranges from -36 ppm [17] to -51 ppm [18]. The calculated magnetostriction constant λ_{100} for CFO is -190 ppm (-252 ppm) for “setting” 1 (3) within GGA+ U , also in reasonably good agreement with experimental results ranging from -225 ppm [19] to -590 ppm [17].

4. Summary

We have presented a detailed first principles study of the structural and magnetic properties of spinel ferrites CFO and NFO, with special emphasis on the usefulness of different exchange-correlation functionals towards a good description of the structural and magnetic properties of bulk and strained structures. Furthermore, we have discussed the influence of strain on the MAE and determined the magnetostriction constants λ_{100} for both CFO and NFO. It has been found that the “+ U ” approach is necessary to obtain a good description of both structural and electronic properties of spinel ferrites, yielding a good quantitative agreement with available experimental data, in particular also for the magnetostriction constant λ_{100} . The specific cation arrangement chosen to represent the *inverse* spinel structure has only a minor influence on the investigated properties. In summary, the results presented here provide evidence, that a quantitative description of the structural and magnetoelastic properties of (*inverse*) spinel ferrites is possible within the (LSDA/GGA)+ U approach, which opens the way for further computational studies of these and related materials.

Acknowledgments

The authors wish to acknowledge financial support by Science Foundation Ireland under Ref. SFI-07/YI2/I1051 and computational resources provided by the Trinity Centre for High Performance Computing (TCHPC) and the Irish Centre for High-End Computing (ICHEC).

References

- [1] Ramesh R and Spaldin N A 2007 *Nature Mat.* **6** 21
- [2] Lüders U, Bibes M, Bobo J F, Cantoni M, Bertacco R and Fontcuberta J 2005 *Phys. Rev. B* **71** 134419
- [3] Huang W, Zhu J, Zeng H Z, Wei X H, Zhang Y and Li Y R 2006 *Appl. Phys. Lett.* **89** 265206
- [4] Lisfi A *et al.* 2007 *Phys. Rev. B* **76** 054405
- [5] Brabers V A M 1995 (*Handbook of Magnetic Materials* vol 8) ed Buschow K H J (Elsevier) pp 189 – 324
- [6] Pénicaud M, Siberchicot B, Sommers C B and Kübler J 1992 *J. Mag. Mag. Mater.* **103** 212
- [7] Antonov V N, Harmon B N and Yaresko A N 2003 *Phys. Rev. B* **67** 024417
- [8] Kresse G and Furthmüller J 1996 *Comput. Mat. Sci.* **6** 15
- [9] Kresse G and Joubert D 1999 *Phys. Rev. B* **59** 1758
- [10] Dudarev S L, Botton G A, Savrasov S Y, Humphreys C J and Sutton A P 1998 *Phys. Rev. B* **57** 1505
- [11] Ederer C and Spaldin N A 2005 *Current Opinion in Solid State and Materials Science* **9** 128
- [12] Rabe K M 2010 *Annu. Rev. Condens. Matter Phys.* **1** 211
- [13] Li Z, Fisher E S, Liu J Z and Nevitt M V 1991 *J. Materials Science* **26** 2621
- [14] Perron H *et al.* 2007 *J. Phys.: Condens. Matter* **19** 346219
- [15] Kittel C 1949 *Rev. Mod. Phys.* **21** 541
- [16] Fritsch D and Ederer C 2010 *Phys. Rev. B* **82** 104117
- [17] Bozorth R M, Tilden E F and Williams A J 1955 *Phys. Rev.* **99** 1788
- [18] Smith A B and Jones R V 1966 *J. Appl. Phys.* **37** 1001
- [19] Chen Y *et al.* 1999 *IEEE Trans. Magn.* **35** 3652